



ORIGINAL ARTICLE

# Feasibility of stereotactic MRI-based image guidance for the treatment of vascular malformations: a phantom study

Marius Schwalbe<sup>1</sup> · Axel Haine<sup>2</sup> · Marc Schindewolf<sup>2</sup> ·  
Hendrik von Tengg-Kobligk<sup>3</sup> · Tom Williamson<sup>1</sup> · Stefan Weber<sup>1</sup> ·  
Iris Baumgartner<sup>2</sup> · Torsten Fuss<sup>2</sup>

Received: 28 December 2015 / Accepted: 5 May 2016 / Published online: 27 May 2016  
© CARS 2016

## Abstract

**Purpose** Treatment of vascular malformations requires the placement of a needle within vessels which may be as small as 1 mm, with the current state of the art relying exclusively on two-dimensional fluoroscopy images for guidance. We hypothesize that the combination of stereotactic image guidance with existing targeting methods will result in faster and more reproducible needle placements, as well as reduced radiation exposure, when compared to standard methods based on fluoroscopy alone.

**Methods** The proposed navigation approach was evaluated in a phantom experiment designed to allow direct comparison with the conventional method. An anatomical phantom of the left forearm was constructed, including an independent control mechanism to indicate the attainment of the target position. Three interventionalists (one inexperienced, two of them frequently practice the conventional fluoroscopic technique) performed 45 targeting attempts utilizing the combined and 45 targeting attempts utilizing the standard approaches.

**Results** In all 45 attempts, the users were able to reach the target when utilizing the combined approach. In two cases, targeting was stopped after 15 min without reaching the target when utilizing only the C-arm. The inexperienced user was faster when utilizing the combined approach and applied

significantly less radiation than when utilizing the conventional approach. Conversely, both experienced users were faster when using the conventional approach, in one case significantly so, with no significant difference in radiation dose when compared to the combined approach.

**Conclusions** This work presents an initial evaluation of a combined navigation fluoroscopy targeting technique in a phantom study. The results suggest that, especially for inexperienced interventionalists, navigation may help to reduce the time and the radiation dose. Future work will focus on the improvement and clinical evaluation of the proposed method.

**Keywords** Stereotactic image guidance · Vascular malformations · MR imaging · Percutaneous needle insertions

## Introduction

Minimally invasive treatment of vascular malformations requires the accurate placement of a catheter or needle to allow the delivery of coils or sclerosants such as ethanol or aethoxysklerol for the subsequent closure of the malformation. In order to avoid ischemic and cardiopulmonary complications, the intervention is performed under general anesthesia and often multiple sessions are needed for complete treatment.

During the needle or catheter placement, the interventionalist utilizes digital subtraction angiography (DSA, a form of fluoroscopic imaging in which a precontrast mask is subtracted from standard angiographic images) for fine targeting or confirmation of the placement of the needle within the vessel. Since only natural high contrast structures, e.g., bone, metal, or calcification, can be visualized, blood is only visible with the use of extrinsic iodinated contrast agent. The initial, rough, targeting of the vessel is performed based on

✉ Marius Schwalbe  
marius.schwalbe@artorg.unibe.ch

<sup>1</sup> ARTORG Center for Biomedical Engineering Research, University of Bern, Bern, Switzerland

<sup>2</sup> Division of Clinical and Interventional Angiology, Inselspital, Bern University Hospital, Bern, Switzerland

<sup>3</sup> Institute of Diagnostic, Interventional and Pediatric Radiology, Inselspital, Bern University Hospital, Bern, Switzerland

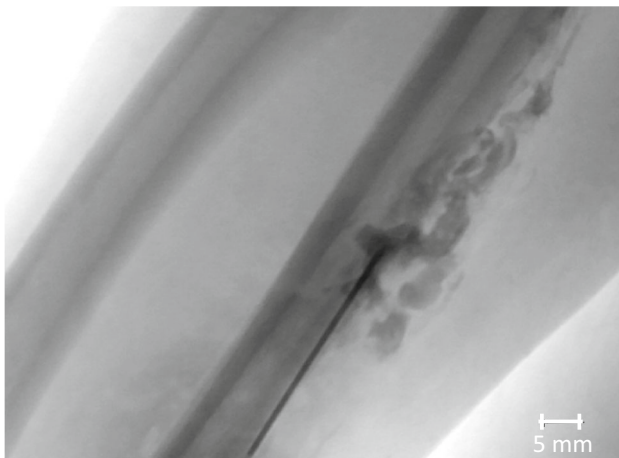


**Fig. 1** Fluoroscopic image of a venous malformation. Contrast agent is injected through a needle inside one of the vessels

the interventionalist's knowledge of the anatomical situation gained from preoperative MRI and ultrasound (US). If US is performed preoperatively, it may be used to mark the skin at needle entry sites, and if used intra-operatively it provides feedback for targeting. However, US assistance is not always practical, for example, in cases of deep lying vessels or sites with difficult US access.

This reliance on angiography leads to increased radiation exposure for both the patient and physician, as well as potentially high volumes of injected contrast agent. Additionally, as fluoroscopic images are only available in 2D, the ability of the interventionalist to orient themselves spatially within the target site can be extremely challenging. Furthermore, malformations of this type, including arteriovenous (AVM) or venous malformations (VM), often manifest themselves as a network of small vessels with diameters of less than 1 mm (see Fig. 1). Limited spatial orientation and the small size of the target vessels can render intervention outcome and duration unpredictable, particularly in complex cases [1].

A number of methods have been proposed toward the improvement of the existing clinical workflow. These can be roughly divided into stereotactic image guidance methods, in which a conventional spatial tracking system (typically optical or electromagnetic) is deployed to allow real-time tracking of an interventional instrument, and nonstereotactic image-guided methods where a visual control loop is closed directly via the utilization of real-time intra-operative imaging.

With respect to nonstereotactic image guidance, a number of studies have been published utilizing various imaging modalities. In [2], low-flow vascular malformations were treated in 19 patients (24 procedures) using a percutaneous sclerosis under direct sonography and fluoroscopy guidance. While the authors claim successful treatment by reducing the number of needle passes, they reported problems

with visibility of needles in sonography images. In [3,4], a nonstereotactic intra-operative MRI-guided approach was suggested as an alternative for low-flow malformations; the authors reported successful treatment in all cases.

In [5], the achievable accuracy when targeting head and neck vascular malformations and tumors (including VM, AVM, and others in total 65 punctures in 27 patients) under the supervision of intra-operative cone beam CT (CBCT) imaging was investigated. The study demonstrated an available accuracy level of around 2 mm when utilizing CBCT guidance. Furthermore, the authors argue that the approach provides guidance for highly accurate needle placement but also mention that the use of a non workflow optimized navigation system is suboptimal with respect to overall intervention time.

With respect to stereotactic guidance, [6] combined a conventional neuro-navigation system (Brainlab, Feldkirchen, Germany) with an interstitial laser system for the treatment of venous malformations in the head and neck region and based on preoperative MR and CT images. While the work is not conclusive about the number of patients treated, authors claim that this approach was supportive in diminishment of tumor volume and the perioperative safety.

For the surgical treatment of intracranial VM/AVM, neuronavigation systems have—like in other neurosurgical applications—become the gold standard. To this end [7,8] both investigated the use of 3D ultrasound-based navigation (SonoWand, Trondheim, Norway) for AVM neurosurgery: The approach helps to understand the vascular structure but [7] also states that the system provides insufficient sensitivity for resection control. Similarly [9–11], utilized standard neuronavigation systems (Medtronic, Dublin, Ireland and Brainlab, Feldkirchen, Germany) for resection guidance of cerebral AVMs based on intra-operative CT imagery and report effective and accurate navigation.

More recently, stereotactic guidance systems have become available for percutaneous interventions, particularly on soft solid organs such as the liver. Such systems are typically optimized for planning, placement, and verification of one or more needle like instruments (i.e., ablation device) and can also be utilized in an interventional setting [12–14].

To our knowledge, no literature is available on the use of stereotactic guidance in the minimally invasive needle-based treatment of distal VM/AVM supported by either MR, CT, or CT-Angio imaging. We believe that the use of stereotactic navigation could help to reduce the major challenges in the treatment of these malformations, particularly those related to spatial orientation within the target site. Note that as the diameter of the vessels to be targeted may be too small for reliable targeting utilizing only navigation, we propose here a combined approach in which navigation is used for the initial placement of the needle within the immediate vicinity of the target, with the endovascular inter-

ventionalist then proceeding under fluoroscopic guidance if necessary.

We hypothesize that the utilization of an stereotactic image guidance system based on preoperative MR images in combination with existing targeting methods will result in faster and more reproducible needle placements and as well as in reduced radiation exposure when compared to standard AVM or VM procedures.

In this study, we report on an experiment aimed at comparing the proposed hybrid approach with state-of-the-art fluoroscopic guidance techniques. The development of a suitable phantom which mimics the interventional situation and provides independent feedback on the attainment of the target is described, as well as experiments evaluating the usability of the proposed method and differences in clinically relevant parameters.

## Materials and methods

### Anatomical phantom for peripheral vascular malformation targeting

The proposed navigation approach was evaluated in a phantom experiment designed to allow direct comparison with the conventional approach based on fluoroscopy. An anatomical phantom of the left forearm was constructed at a 1:1 scale based on obtained imaging data, with the inclusion of an independent control mechanism (i.e., neither navigation nor fluoroscopy) to indicate the attainment of the target position. The construction of the phantom is described in detail in the following section (see Fig. 2).

### Imaging protocol and 3D modeling

Preoperative MRI scans of the lower left arm of a patient diagnosed with VM were selected to build the patient-specific phantom. The MRI sequences used for building the targeting phantom include a coronal contrast-enhanced time-resolved gradient echo sequence (matrix size = 448 × 364 × 80,

TR = 3.10 ms, TE = 1.16 ms) with an isotropic resolution of 1 mm and a coronal contrast-enhanced fat saturated steady-state gradient echo sequence (matrix size = 448 × 364 × 96, TR = 6.44 ms, TE = 3.00 ms) with pixel size of 0.89 mm and slice thickness of 1.1 mm.

Semiautomatic segmentation was performed to extract the patient anatomical structure using Amira (Zuse Institute Berlin, Germany). The bones and the skin were segmented using thresholding and manual selection from the coronal gradient echo sequence. In addition, the VM was manually segmented from the fat saturated MRI sequence, to get an understanding for a realistic placement of the targets in the phantom.

The segmentation was subsequently rendered into 3D meshes. The upper surface of the skin was then removed using MeshMixer (Autodesk, San Rafael, California, USA) to provide an open space for needle insertion.

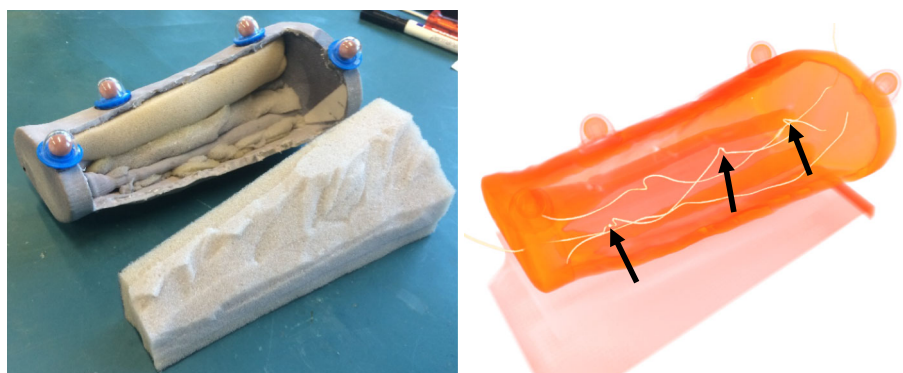
### Construction

The 3D model of the skin and the bones was then rapid prototyped using a 3D printer (Spectrum Z<sup>TM</sup>510, 3D Systems, Rock Hill, South Carolina, USA). To simulate vessels and targets within the region of interest from the segmented MR images, a wire with a diameter of 3 mm was used. The jacket was removed from the cable in three places and a knot tied to represent the target (see Fig. 3 for a detailed illustration of the targets).

The cable was then connected to a battery pack; upon contact with the target by the tip of the needle, the electrical loop is closed and an LED inside the needle lights up (see Fig. 4). Finally, the opening of the skin surface was closed by filling foam, mimicking the muscle in the arm.

Four single markers (SM) were attached to the phantom, allowing tracking by the navigation system. As neither the single markers nor any of the materials utilized in the construction of the phantom can be imaged using MRI, a CT scan of the phantom was performed to allow the acquisition of the position of the markers relative to the artificial vessel

**Fig. 2** Left the rapid prototyped phantom with the four single markers attached. The targets are inserted into the block of foam and the foam then glued into the phantom. Right volume rendering of the CT scan of the phantom. The three targets are indicated by the arrows



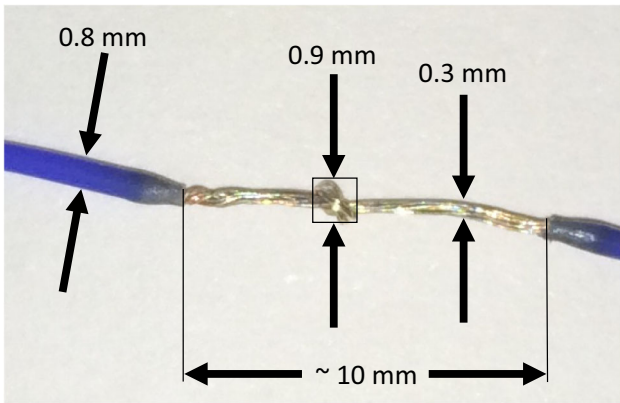


**Fig. 3** The dimensions of the targets: It consists of a cable where approximately 10 mm are stripped. The diameter of the stripped wire is 0.3 mm. In the middle of the stripped part, there is a *knot*, which is the actual target. This *knot* is visible in CT as well as in the fluoroscopy

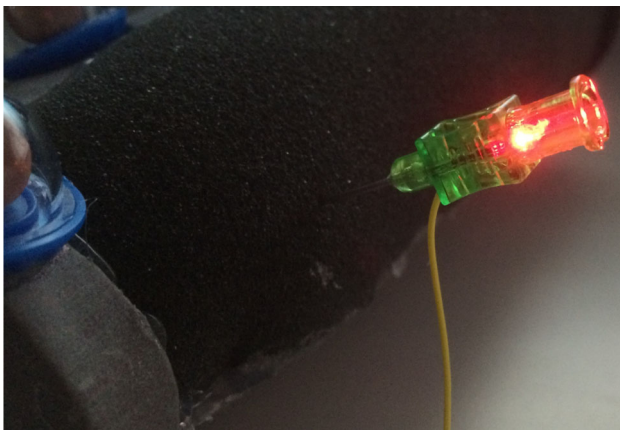


**Fig. 4** Illuminated LED inside the needle, indicating that the tip of the needle is at a target inside the phantom. The shaft of the needle is coated, so that just a contact with the tip of the needle is able to close the electrical loop

targets. In a clinical scenario, MRI-compatible markers will be used and no preoperative CT scan is required.

## Experimental evaluation of proposed approach

### Stereotactic navigation system

An existing surgical navigation system (CAS-One Vario, CAScination, Bern, Switzerland) developed for open liver surgery [15] and interventional procedures [16] was adapted to the requirements of percutaneous needle insertions for VM treatment. Tracking of surgical tools is completed by means of an optical tracking system (NDI Polaris Vicra, Northern Digital, Waterloo, Ontario, Canada) and a set of custom marker shields with passive markers which can be adapted to a variety of instruments.

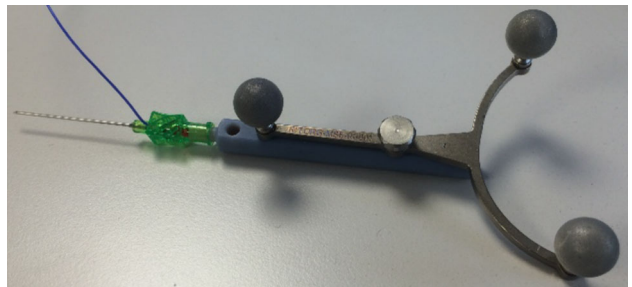


**Fig. 5** The needle equipped with a cable and a LED inside, attached to the adapter to connect the marker shield for the optical tracking of the needle

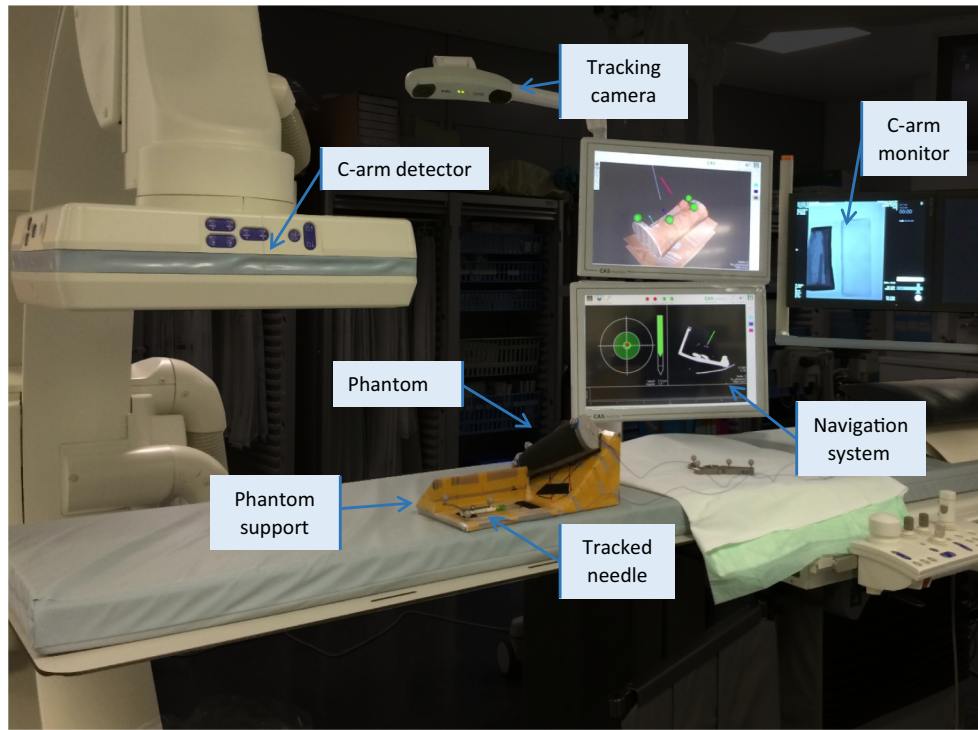
For targeting a 21G Chiba-tip needle was equipped with an adapter and an existing marker shield attached to the needle adapter (see Fig. 5). After marker attachment of the needle is calibrated using a multicalibration unit (MCU) with an inlay to insert the needle in a predefined position, and the transformation from the tip of the needle to the attached marker shield derived.

Image-to-phantom registration and tracking of the patient rely on biocompatible, sterilizable, single reflective marker spheres, glued to the phantom prior to CT imaging. These spheres are visible in CT image data and can be tracked intra-operatively, thereby allowing the automatic registration of the patient to preoperative image data and real-time updates to this transformation. Registration accuracy can be checked visually by examining the alignment of tracked and preoperative marker positions in a rendering of the surgical scene provided by the navigation software.

### Experimental workflow

To evaluate the effectiveness of the proposed combined navigation-fluoroscopy approach with respect to the conventional procedure using only the C-arm, a comparative experiment was designed. Three interventionalists from the Division of Clinical and Interventional Angiology at the Bern University Hospital (angiologists, two of them frequently practice vessel targeting with needles under fluoroscopy) were asked to perform the targeting procedure in the developed phantom using both the standard approach and with the support of the navigation system (see Fig. 6). The experiments were performed on different days without observation by the other users.

Since a VM can occur in nearly all parts of the body and the patient cannot always be positioned such that the region of interest is easily accessible, the phantom was placed onto a support in five different positions and orientations. In each of these positions, the three targets contained within the phantom were then targeted using the conventional and the hybrid method. The order of the phantom position, specific



**Fig. 6** The experimental setup of the phantom study

target and targeting method was pseudorandomized for each interventionalist to ensure that the same target or phantom position was not repeated in subsequent trials. The attempts with and without navigation were alternated giving a total of 30 attempts (2 methods, 5 positions, 3 targets) for each user (an overview of the workflow can be seen in Fig. 7).

Prior to the experiments, the users were instructed verbally in the use of the navigation system as well as being allowed 15 min for familiarization with the systems and the setup. For each needle insertion, the time to reach the target was recorded for both approaches. For each attempt, the dose and the time of radiation from the C-arm was recorded by measuring the summed values given by the system. A restart was possible at any time within the trial and at the discretion of the operator. The trial was stopped if the target was not reached after 15 min and marked as failed.

Additionally, each user was asked to complete a questionnaire at the end of the experiment about the two approaches as well as completing the Standard Usability Scale (SUS) questionnaire regarding the use of the navigation system. The SUS is a widely used standardized 10 item usability questionnaire [17]. The specific questionnaire was developed without the involvement of the test subjects.

#### Conventional targeting approach

In the conventional approach, the task was to target using only the needle and a standard C-arm (Artis Zee, Siemens,

Berlin, Germany). Before each attempt, the C-arm was placed in a neutral position, i.e., the phantom was not visible in the C-arm image and the detectors placed parallel to the OR table. The interventionalist was then instructed to follow the conventional procedure, placing the needle until the target was reached.

#### Combined C-arm/navigation approach

Trajectories were planned from the surface of the phantom skin to each of the targets, and the C-arm was placed in the same neutral position as for the conventional attempts. The interventionalist was then requested to initially place the needle using the navigation system.

The needle was first attached to the marker shield and calibrated; the navigation system then provided feedback to the interventionalist with respect to the lateral and angular errors from the planned trajectory. Additionally, the navigation system indicated when an axial distance of 5 mm before the target was reached. After the initial placement, the interventionalist was free to utilize the system as desired. The decision of whether to continue targeting with navigation and when to detach the needle from the needle holder and perform the final track under fluoroscopic guidance was left to the interventionalist.

Since the optical tracking camera is mounted onto the stand of the navigation system, the position of the camera cannot be adapted in height. Therefore, it is not possible

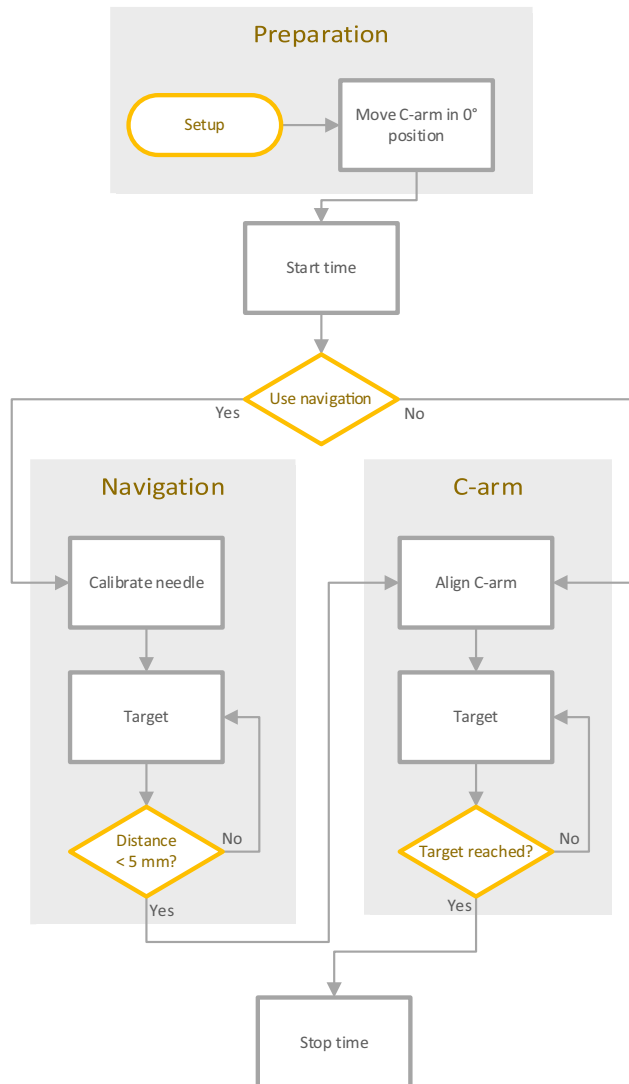


**Fig. 7** The proposed workflow

to use the navigation, when the C-arm is placed over the phantom and vice versa.

### Data analysis

Data were analyzed using MATLAB (MathWorks, Natick, Massachusetts, USA). The mean and standard deviation for the targeting times were computed and compared via the two-tailed, two-sample *t* test ( $p=0.05$ ) grouped by the system (inter-system), the users (inter-user), and the attempts (intra-user).

The feedback of the interventionalists was evaluated with a questionnaire. Each of the subjects was asked if they were confident reaching the target, if they found it frustrating to reach the target and in the case of the combined approach if it was feasible to integrate into clinical routine. The responses were rated on a scale from 1–5 (“strongly

**Table 1** Summary of the results for targeting time and radiation dose ( $n=45$ )

	Standard (mean ± std.)	Combined (mean ± std.)
Targeting time (s)	$223 \pm 208$	$223 \pm 178$
Radiation dose ( $\mu\text{Gym}^2$ )	$6.2 \pm 4.2$	$4.6 \pm 5.7$
Failed attempts	2/45	0/45

disagree”—“strongly agree”) for each question. The results from the SUS for the navigation system were evaluated according to the recommended procedure, resulting in a scale from 0–100 in which 0 would be not usable at all and 100 the theoretical maximum. Since all of the users are working at the Bern University Hospital and are aware of the ongoing research, we cannot rule out a bias in the questionnaire.

### Results

The required modifications and development of the required components to allow targeting of peripheral vascular malformations were made to the existing navigation platform. A phantom simulating the desired interventional procedure and provided independent feedback upon attainment of the target was successfully developed.

Each of the 3 interventionalists performed 15 targeting attempts (5 positions and 3 targets) with each of the two approaches, giving a total of 90 attempts. When utilizing the combined navigation/C-arm approach, the users were able to reach the target in all 45 attempts. When utilizing the C-arm only approach, in two cases the targeting was stopped after 15 min without reaching the target.

The required targeting time and radiation dose are summarized in Table 1. On average, users required the same amount of time to reach the target using both approaches, and a lower standard deviation was observed when utilizing the combined approach. On average, users applied less dose when utilizing the combined approach; however, the difference was not significant ( $p=0.14$ , 2-sided *t* test).

In Fig. 8, the data for the time (left) and radiation dose (right) are summarized per user and per approach; note that user 1 is the inexperienced interventionalist, while users 2 and 3 frequently practice vessel targeting with needles under fluoroscopy. The inexperienced user was, on average, faster using the navigation, while the other users were slower, with user 2 significantly faster using the C-arm only approach ( $p = 0.02$ , 2-sided *t* test). Regarding the radiation dose, user 1 required significantly less radiation ( $p = 0.045$ , 2-sided *t* test) when utilizing the combined approach. User 3 also applied less radiation, while user 2 applied slightly

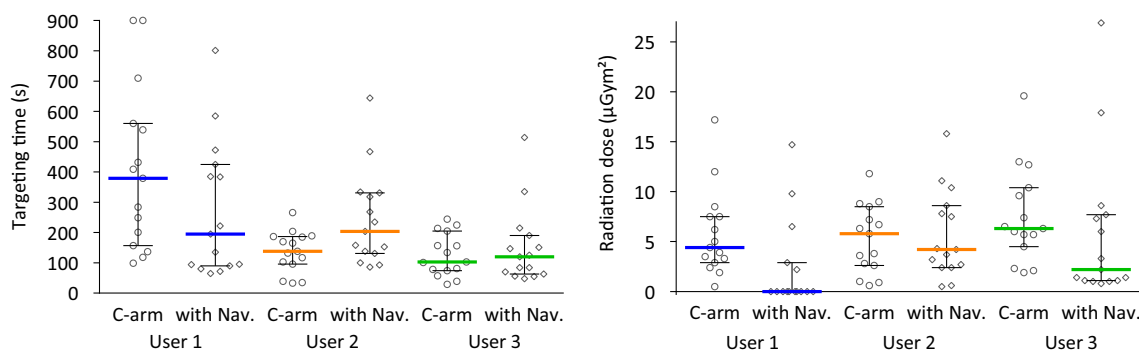
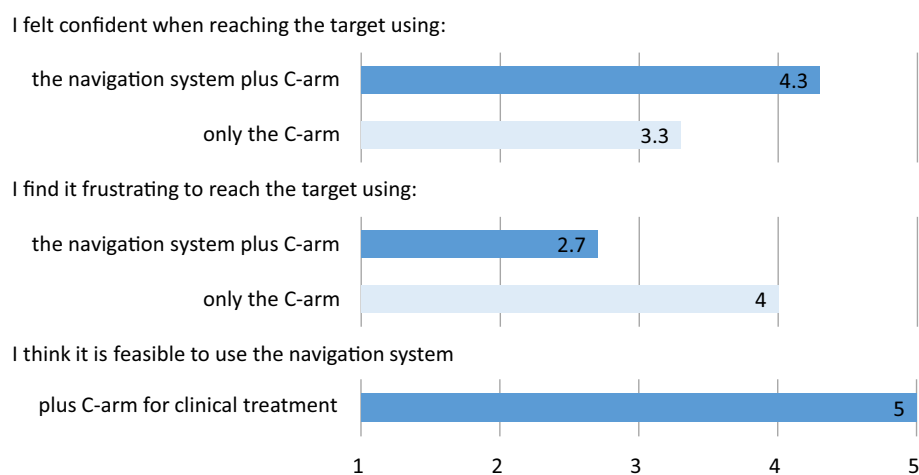


**Fig. 8** Targeting time (left) and Radiation dose (right) needed for targeting for all users without and with navigation. The colored bars show the medians of the values and the error bars the quartiles

**Fig. 9** Summary of the questionnaire response results ( $n=3$ , from 1 strongly disagree to 5 strongly agree)



more during the navigated attempts; neither difference can be considered as significant.

The results of the questionnaire are summarized in the bar chart (Fig. 9). It can be seen that the users felt more confident when reaching the target using the combined approach, while at the same time they find it less frustrating (both differences are not significant:  $p = 0.1$  and  $p = 0.37$ ). Moreover, all three interventionalists strongly agree that they think it is feasible to use the navigation system with the C-arm for clinical treatment.

The Standard Usability Scale (SUS) regarding the navigation system in the combined C-arm/navigation approaches resulted in a score of 90. The question with the lowest rating (5.8 of 10 points) was question number four: two of the three users (the inexperienced and one of the two experienced users) reported that they would need initial support from a technical person to be able to use the system.

## Discussion

Presented above is an initial experimental evaluation of stereotactic navigation for the treatment of peripheral vas-

cular malformations. An anatomical phantom mimicking the real interventional situation was developed and a new combined technique for performing percutaneous vascular targeting assessed in comparison with the existing state-of-the-art methods by three angiologists.

The percutaneous targeting of vascular structures is a highly challenging procedure requiring physicians to reach structures as small as 1 mm relying only on 2D fluoroscopic images for orientation within the region of interest. Stereotactic navigation may help to improve spatial orientation through the feedback of position within a virtual scene based on preoperatively obtained image data; however, the accuracy of these systems is limited. Subsequently, although it may not be possible to reliably target structures of this scale using navigation alone, we hypothesized that the use of navigation in combination with existing techniques could lead to improved targeting times as well as reduced radiation dose. The presented technique can be utilized as an alternative to, or in combination with, the utilization of pre- or intra-interventional ultrasound, as well as allowing more accurate initial needle placement in cases in which ultrasound imaging is of limited use, such as deep lesions. The approach may also be useful in cases in which the

interventionalist is not experienced with the use of ultrasound.

The techniques utilized, and results observed, among each of the physicians varied quite significantly. Differences between the inexperienced interventionalist and the users who frequently practice vessel targeting with needles under fluoroscopy were particularly prominent. The inexperienced user (user 1) was significantly slower when utilizing the standard approach relying on only the C-arm and failed to reach the target in two cases (the targeting was stopped after 15 min). Due to the inexperience with the C-arm, when provided with the opportunity for the use of navigation he used it extensively and was able to target with the navigation in 10 of 15 cases without using the C-arm.

Independently, one of the experienced interventionists (user 2) attempted the same approach, but failed in all 15 attempts to just target based purely on navigation. This resulted in a much longer targeting time using the navigation, performing multiple targeting attempts with navigation and only eventually switching to the C-arm. The second experienced user (user 3) took a different approach, using the navigation for the initial placement of the needle and then immediately switching to the C-arm resulting in reduced radiation dose when utilizing the navigation system; however, the time needed was slightly longer. This was likely caused by two major factors: extensive experience operating the C-arm, as opposed to integrating the additional information provided by the navigation system, and the time required to switch from the navigation system to the C-arm.

Overall, the results suggest that the radiation dose required for targeting of vascular malformations can be reduced through the integration of stereotactic image guidance methods, particularly in the case of inexperienced users. Furthermore, for inexperienced users, the targeting time can be reduced by integrating a navigation system into the workflow. It remains unclear if this will be also the case for experienced users, particularly if they gain more experience using the navigation system and the most effective methods for combining the two methods. The skill of the two experienced users is reflected in the targeting times, requiring on average only 126 and 137 s, respectively. The achievement of targeting times at this level is difficult when using two systems which cannot be used simultaneously, and where the navigation needle needs to be calibrated beforehand.

This study aims to go beyond a standard navigation accuracy study by providing a clinically relevant experimental setup and workflow. The developed phantom provides a relatively realistic simulation of the interventional situation; it has the advantage of providing an independent indication of target attainment, while also preventing positioning of the needle based on haptic feedback through the use of cables instead of rigidly fixed targets. The developed phantom does, however, have a number of limitations; while the use of foam

simulates the nonrigidity observed in real clinical interventions, it does not cover the full range of deformation possible in some areas of the body. Furthermore, as the reference markers were fixed to the rigid portion of the phantom, deformation did not affect the patient-to-image registration as it would in reality. Finally, it remains an open question if the fast targeting with only the C-arm can be accounted to the limited complexity of the phantom: In the fluoroscopic images, the targets are clearly visible at any time, which is not the case for a real blood vessel. This may somewhat compromise the results against the combined approach, as the movement of the targets caused by the approaching needle is visible under fluoroscopy and not with the navigation.

The proposed workflow is based on the limitations of stereotactic navigation systems with respect to the achievable accuracy during targeting. In the specific case of needle-based interventions, the nonrigidity of the target organ relative to the preoperative image data and the bending of the needle upon insertion add significantly to the inaccuracy beyond standard navigation errors such as tracking and registration. Subsequently, until the accuracy of navigation can be improved, reliable targeting of small structures with navigation alone is not feasible. Improvements in accuracy may be possible through the use of electromagnetic tracking instead of optical; this would allow tracking of the needle directly at the tip, thereby removing errors due to needle bending. The use of electromagnetic tracking, however, would require the investigation of new methods for registration and tracking of the patient. Finally, it was not possible to use the C-arm and the navigation at the same time due to the location of the tracking system, prolonging the workflow when using the combined approach. This drawback may be overcome by placing the tracking camera on a separate stand. One further limitation of the approach is the requirement for an additional MR scan performed shortly before the intervention time. Subsequently, markers for navigation need to be present in the image and the patient position should be equal to the position during the intervention.

Each of the physicians strongly agreed that the use of navigation for clinical treatment is feasible. Note, however, that this positive feedback may be a projection toward the potential capabilities of the approach rather than a specific recommendation to use the system as it currently is. Preparation for an initial clinical evaluation utilizing the proposed technique is currently underway. We anticipate that the system can be integrated into the clinical setup in the interventional suite as in this study; however, adjustments to the preoperative imaging workflow are required. Since MRI is the main imaging modality for diagnostic workup and treatment planning for vascular malformations, the navigation in a real clinical scenario will be based on the MR images, so no additional radiation is applied. As the current retroreflective markers for the navigation are intended

for CT-based interventions and are made out of solid plastic, they are not visible in MRI. To overcome this limitation, the markers will be filled with oil prior to imaging, allowing their detection in the MR images. The clinical workflow for the use of oil-filled markers will require the use of a template: The desired marker positions will be drawn onto the skin, and subsequently, the MRI-compatible spheres will be placed at these positions. The oil-filled markers will then be removed after imaging, and a set of sterile markers for the intra-operative portion of the procedure will be placed at the required positions. Initial imaging and workflow tests using MRI and the filled markers demonstrated the feasibility of this process.

## Conclusions

Presented above is the integration of an interventional stereotactic image guidance system into the workflow for minimally invasive needle-based treatment of distal venous malformations. The initial results utilizing the combined navigation fluoroscopy targeting technique show that, especially for inexperienced interventionalists, the navigation helps to reduce the time and the radiation dose. Future work will focus on the improvement and clinical evaluation of the proposed method.

**Acknowledgments** The work presented in this manuscript was partially funded by the Ruth & Arthur Scherbarth Stiftung. The authors would like to acknowledge Huanxiang Lu, Matteo Fusaglia, Denise Baumann, Matthias Peterhans, and Juan Ansó for advice, and CAScination AG for providing the IGS system used in the experiments.

## Compliance with ethical standards

**Conflict of interest** The authors declare that they have no conflict of interest.

**Human and animal rights** This article does not contain any studies with human participants or animals performed by any of the authors.

## References

- Yakes W, Baumgartner I (2014) Interventional treatment of arteriovenous malformations. *Gefässchirurgie* 19(4):325–330
- Donnelly LF, Bissett GS, Adams DM (1999) Combined sonographic and fluoroscopic guidance: a modified technique for percutaneous sclerosis of low-flow vascular malformations. *Am J Roentgenol* 173(3):655–657
- Andreisek G, Nanz D, Weishaupt D, Pfammatter T, Imaging-guided MR (2009) Percutaneous sclerotherapy of peripheral venous malformations with a clinical 1.5-T unit: a pilot study. *J Vasc Interv Radiol* 20(7):879–887
- Lewin JS, Merkle EM, Duerk JL, Tarr RW (1999) Low-flow vascular malformations in the head and neck: safety and feasibility of MR imaging-guided percutaneous sclerotherapy—preliminary experience with 14 procedures in three patients. *Radiology* 211(2):566–570
- Nesbit GM, Nesbit EG, Hamilton BE (2011) Integrated cone-beam CT and fluoroscopic navigation in treatment of head and neck vascular malformations and tumors. *J Neurointerv Surg* 3(2):186–190
- Hoffmann J, Westendorff C, Troitzsch D, Ernemann U, Reinert S (2004) Image-guided navigation for the control interstitial laser therapy of vascular malformations in the head and neck region. *Biomedical engineering* 49(7–8):199–201
- Mathiesen T, Peredo I, Edner G, Kihlström L, Svensson M, Ulfarsson E, Andersson T (2007) Neuronavigation for arteriovenous malformation surgery by intraoperative three-dimensional ultrasound angiography. *Neurosurgery* 60(4 SUPPL. 2):345–351
- Unsgaard G, Ommedal S, Rygh OM, Lindseth F (2005) Operation of arteriovenous malformations assisted by stereoscopic navigation-controlled display of preoperative magnetic resonance angiography and intraoperative ultrasound angiography. *Neurosurgery* 56(4 SUPPL.):281–290
- Raza SM, Papadimitriou K, Gandhi D, Radvany M, Olivi A, Huang J (2012) Intra-arterial intraoperative computed tomography angiography guided navigation: a new technique for localization of vascular pathology. *Neurosurgery* 71(SUPPL.2):240–252
- Coenen VA, Dammert S, Reinges MHT, Mull M, Gilsbach JM, Rohde V (2005) Image-guided microneurosurgical management of small cerebral arteriovenous malformations: the value of navigated computed tomographic angiography. *Neuroradiology* 47(1):66–72
- Muacevic A, Steiger HJ (1999) Computer-assisted resection of cerebral arteriovenous malformations. *Neurosurgery* 45(5):1164–1171
- Toporek G, Wallach D, Weber S, Bale R, Widmann G (2013) Cone-beam computed tomography-guided stereotactic liver punctures: a phantom study. *Cardiovasc Interv Radiol* 36(6):1629–1637
- Widmann G, Wallach D, Toporek G, Schullian P, Weber S, Bale R (2013) Angiographic C-arm CT-versus MDCT-guided stereotactic punctures of liver lesions: nonrigid phantom study. *Am J Roentgenol* 201(5):1136–1140
- Koethe Y, Xu S, Velusamy G, Wood BJ, Venkatesan AM (2014) Accuracy and efficacy of percutaneous biopsy and ablation using robotic assistance under computed tomography guidance: a phantom study. *Eur Radiol* 24(3):723–730
- Peterhans M, Berg A, Dagon B, Inderbitzin D, Baur C, Candinas D, Weber S (2011) A navigation system for open liver surgery: design, workflow and first clinical applications. *Int J Med Robot Comput Assist Surg* 7(1):7–16
- Wallach D, Toporek G, Weber S, Bale R, Widmann G (2014) Comparison of freehand-navigated and aiming device-navigated targeting of liver lesions. *Int J Med Robot Comput Assist Surg* 10(1):35–43
- Brooke J (1996) SUS—a quick and dirty usability scale. *Usability Eval Ind* 189(194):4–7